Stability, Causality, and Passivity in Electrical Interconnect Models

Stability, Causality, and Passivity in Electrical Interconnect Models

Piero Triverio, *Student Member, IEEE*, Stefano Grivet-Talocia, *Senior Member, IEEE*, Michel S. Nakhla, *Fellow, IEEE*, Flavio G. Canavero, *Fellow, IEEE*, and Ramachandra Achar, *Senior Member, IEEE*

***Abstract*—Modern packaging design requires extensive signal integrity simulations in order to assess the electrical performance of the system. The feasibility of such simulations is granted only when accurate and efficient models are available for all system parts and components having a significant influence on the signals. Unfortunately, model derivation is still a challenging task, despite the extensive research that has been devoted to this topic. In fact, it is a common experience that modeling or simulation tasks sometimes fail, often without a clear understanding of the main reason. This paper presents the fundamental properties of causality, stability, and passivity that electrical interconnect models must satisfy in order to be physically consistent. All basic definitions are reviewed in time domain, Laplace domain, and frequency domain, and all significant interrelations between these properties are outlined. This background material is used to interpret several common situations where either model derivation or model use in a computer-aided design environment fails dramatically. We show that the root cause for these difficulties can always be traced back to the lack of stability, causality, or passivity in the data providing the structure characterization and/or in the model itself.**

***Index Terms*—Bilateral Laplace transform, causality, dispersion relations, high-speed interconnects, linear systems, modeling, passivity, stability.**

I. Introduction

THE design of modern high-speed digital or mixed-signal packaged systems calls for automated and robust modeling and simulation tools [1], [2]. Any system component or interconnect that has some influence on the quality of the signals must be accurately characterized and modeled over a broad frequency band so that its signal degradation effects can be assessed via system-level simulations. Despite the extensive research work that has been devoted to model extraction for passive components and interconnects [3]–[14], this remains a very challenging task. This is partly due to the ever increasing bandwidth that is required for the characterization of the structure and partly to the overall system complexity, both in terms of number of components and fine geometrical details.

A common strategy that is employed for model extraction is based on a two-step procedure. First, the frequency-domain responses of a given structure are obtained via direct measurement or simulation. Examples can be the scattering matrix of some electrical interconnect or the impedance of a power/ground distribution network. This first step leads to a set of tabulated frequency responses of the structure under investigation. Then, a suitable identification procedure is applied to extract a model from the above tabulated data. This second step aims at providing a simplified mathematical representation of the input–output system behavior, which can be employed in a suitable simulation computer aided-design (CAD) environment for system analysis, design, and prototyping. For instance, rational macromodels are highly desirable for electrical interconnects since they can be easily synthesized as SPICE netlists. References [3]–[14] provide an overview of the most prominent model extraction techniques for electrical interconnects and package structures.

One of the key points in the above-described procedure is accuracy preservation during the model extraction. Obviously, the designer needs accurate models for a sound representation of the electrical behavior of the system. However, accuracy is not the only and not even the most important feature for assessing the quality of a model. One of the purposes of this paper is indeed to show that more fundamental properties must be guaranteed. What is really relevant under a practical standpoint is the physical consistency of the final model, which can be compromised in any of the above two steps. Measurement errors or numerical simulation inaccuracies can lead to poor system specifications in frequency domain (first step), which in turn will impair any subsequent modeling attempt. Nonetheless, even advanced state-of-the-art modeling algorithms (second step) may have some weakness which might produce inconsistent models even when the original data specification is good.

Any model must be characterized by the same basic physical properties of the structure that it should represent. In this paper, we concentrate on linear systems that are intrinsically stable, causal, and passive, such as electrical interconnects and passive components. We will show that when the frequency-domain characterization (obtained via direct measurement or simulation) of the structure lacks one or more of these properties, several inconsistencies may arise, leading to a possible failure of the signal integrity assessment. It should be noted that stability, causality, and passivity are often assumed blindly by the practitioner or even by the highly trained engineer, who may be unaware of the true reason for the failure of some analysis/design task making use of flawed models.

In this paper, the fundamental properties of stability, causality, and passivity are reviewed, and several results on their interrelations are presented. Although most of the material is not new, we cast all fundamental properties in a form that is suitable to interpret a few common situations (mainly in the

Manuscript received August 13, 2006; revised April 9, 2007.

P. Triverio, S. Grivet-Talocia, and F. G. Canavero are with the Department of Electronics, Politecnico di Torino, Torino 10129, Italy (e-mail: piero.triverio@polito.it; stefano.grivet@polito.it; flavio.canavero@polito.it).

M. S. Nakhla and R. Achar are with the Department of Electronics, Carleton University, Ottawa, ON K2S-5B6, Canada (e-mail: msn@doe.carleton.ca; achar@doe.carleton.ca).

Digital Object Identifier 10.1109/TADVP.2007.901567

field of electrical interconnect and packaging) where model derivation and/or model use in a CAD simulation environment fail. Section II presents an example of such a scenario, providing additional motivation for this tutorial paper.

We review the basic time-domain definitions of causality, stability, and passivity in Section III. Section IV analyzes the implications of these three properties in the Laplace domain, which is the most natural domain for an in-depth theoretical analysis. Frequency domain conditions are then reviewed in Section V. The theoretical presentation is interspersed with several illustrative examples. These examples are deliberately very simple, in order to focus on each specific result during the flow of the presentation. However, a few examples coming from real applications for which modeling or simulation is problematic are presented in Section VI. The theory presented in this paper will provide a straightforward interpretation of these difficulties, by pointing out their root cause. Once this cause is detected, possible countermeasures can be taken, as discussed in the paper and in Section VII.

The theoretical material is presented in a formal way. However, fine mathematical details are often omitted to avoid heavy notations and long derivations. Therefore, most theorems are stated without a proof. Also, most results are presented by assuming that all signals are standard functions of time, although the theory of distributions should be used whenever appropriate. These advanced topics are fully covered in the references.

II. Motivation

This section considers a simple interconnect example for which the generation of a macromodel fails. We present the example under the standpoint of the design engineer, who knows the physical geometry of the interconnect and is required to generate a SPICE-compatible model in order to carry out the design. The structure is a three-conductor transmission line. Its scattering matrix is first computed over a bandwidth of 4 GHz using a commercial frequency-domain 3-D field solver. Then, the various scattering matrix entries are processed by the very popular and robust vector fitting (VF) algorithm [3] in order to produce a lumped model for the structure. It is well known that VF produces a model in poles-residues form, which is readily synthesized into a SPICE netlist. It turns out that VF fails to provide a reasonably accurate model. As an example, we report in Fig. 1 the original return loss S_{11} and the corresponding response of a rational model with 20 poles. Although the raw data are quite smooth, the model is very inaccurate.

The first solution one can think of in order to improve the accuracy is to increase the number of model poles or the number of VF iterations. Table I reports the resulting fitting error for up to 40 poles. The table clearly shows that even if the model order or the number of VF iterations are increased, the accuracy remains poor. The rational fitting scheme does not seem to converge.

The standard VF algorithm avoids the presence of unstable poles by changing the sign of their real part whenever they occur during the iterations. Our next try is to disable this feature and

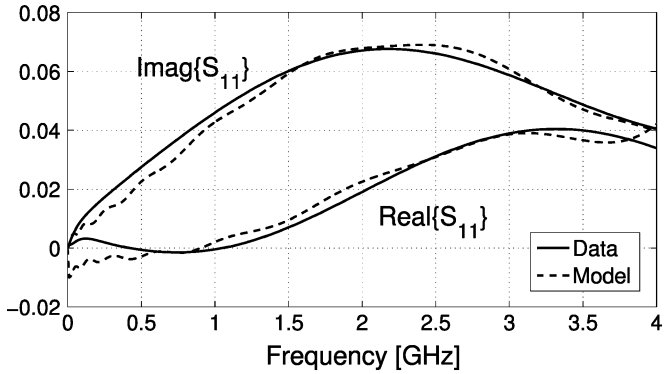

Fig. 1. VF-generated model (20 poles, all with negative real part). Raw S_{11} response (solid line) and model response (dashed line).

TABLE I
Accuracy of the Rational Model Generated by Vector Fitting. Poles With Positive Real Parts Are Not Allowed

Model order	VF iterations	Maximum error
10	4	1.4×10^{-2}
20	4	1.1×10^{-2}
30	4	1.0×10^{-2}
30	15	1.1×10^{-2}
40	15	1.2×10^{-2}

to let VF choose the best poles placement in the entire complex plane. Surprisingly, VF readily computes a highly accurate model even with few poles, as illustrated in Table II. Unfortunately, this model will be useless for any practical purpose because, due to the presence of unstable poles, any time-domain simulation in a CAD environment will blow up exponentially. Moreover, it is quite unreasonable that the frequency response of a certainly passive structure requires the presence of unstable poles for its rational approximation.

It turns out that the raw frequency responses are flawed by causality violations, as we will demonstrate in Section VI. However, the symptoms of these inconsistencies arise only when trying to fit the data. Consequently, the main problem is difficult to identify, and even more difficult is to realize how to fix it. The theoretical results presented in Sections III–V will provide the background material that will allow, in Section VI, a complete explanation and interpretation of the VF results for this example.

III. Time Domain

In this section, the physical concepts of causality, stability, and passivity are described and precisely defined by appropriate mathematical conditions. We restrict our attention to linear[1] and

[1]A system is linear if the response to a linear combination of two inputs

$$\mathbf{x}(t) = c_1\mathbf{x}_1(t) + c_2\mathbf{x}_2(t)$$

is

$$\mathbf{w}(t) = c_1\mathbf{w}_1(t) + c_2\mathbf{w}_2(t)$$

where $\mathbf{w}_1(t)$ and $\mathbf{w}_2(t)$ are the outputs corresponding to each input $\mathbf{x}_1(t)$ and $\mathbf{x}_2(t)$, respectively.

TABLE II
ACCURACY OF RATIONAL MODEL GENERATED BY VF. POLES WITH POSITIVE REAL PARTS ARE ALLOWED

Model order	Stable	Maximum error
10	NO	7.3×10^{-3}
20	NO	1.4×10^{-4}
30	NO	1.2×10^{-4}

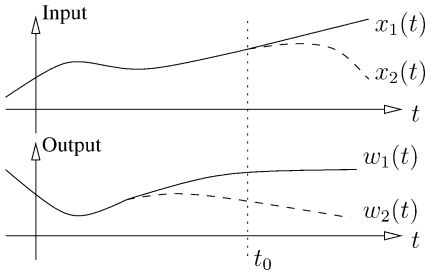

Fig. 2. Example of noncausal system behavior: two inputs $x_1(t)$ and $x_2(t)$, equal up to $t = t_0$, leading to outputs $w_1(t)$ and $w_2(t)$ that differ earlier than $t = t_0$.

time-invariant[2] electrical n-port networks, with input and output denoted, respectively, by the n-element vectors $\mathbf{x}(t)$ and $\mathbf{w}(t)$. Due to linearity and time invariance, the system can be conveniently represented with a convolution [26] relating the input $\mathbf{x}(t)$ and output $\mathbf{w}(t)$,

$$\mathbf{w}(t) = \mathbf{h}(t) * \mathbf{x}(t) = \int_{-\infty}^{+\infty} \mathbf{h}(t-\tau)\mathbf{x}(\tau)\, d\tau. \qquad (1)$$

The matrix $\mathbf{h}(t)$ is the system impulse response, with each element $h_{ij}(t)$ being the response at port i when an ideal impulse (Dirac's delta) is applied at port j, with all other inputs set to zero. We will consider different representations of electrical n-port networks, including impedance ($\mathbf{x}$ being currents and $\mathbf{w}$ voltages), admittance ($\mathbf{x}$ being voltages and $\mathbf{w}$ currents), and scattering (both $\mathbf{x}, \mathbf{w}$ being power waves).

A. Causality

It is part of our real world experience that an effect cannot precede its cause. This intuitive concept is the fundamental principle of causality [33], that every physical system has to respect. For example, if two inputs $\mathbf{x}_1(t)$ and $\mathbf{x}_2(t)$, equal up to $t = t_0$, are applied to a causal system, their respective outputs are expected to be equal up to $t = t_0$. If this is not the case (see Fig. 2), the system is noncausal, because it forecasts a difference in the inputs before it actually occurs.

The precise definition of causal system that follows is just the formal writing of this intuitive consideration.

Definition III.1 (Causality [25]): A system is causal if and only if for *all* input pairs $\mathbf{x}_1(t)$ and $\mathbf{x}_2(t)$ such that

$$\mathbf{x}_1(t) = \mathbf{x}_2(t), \quad t \le t_0 \quad \forall t_0$$

the two corresponding outputs satisfy

$$\mathbf{w}_1(t) = \mathbf{w}_2(t), \quad t \le t_0.$$

[2]The time-invariance property identifies those systems that do not change their behavior with time. If $\mathbf{w}(t)$ is the output excited by input $\mathbf{x}(t)$, then $\mathbf{w}(t-\tau)$ is the output for the delayed input $\mathbf{x}(t-\tau)$.

From this general definition, a simpler condition for the causality of linear systems can be stated [25].

Theorem III.1: A linear system is causal if and only if for every input $\mathbf{x}(t)$ that vanishes for $t < t_0$, the corresponding output $\mathbf{w}(t)$ vanishes too for $t < t_0$.

Finally, we derive the important constraint imposed by causality on the impulse response $\mathbf{h}(t)$ of linear time-invariant (LTI) systems [26].

Theorem III.2: An LTI system is causal if and only if all the elements $h_{ij}(t)$ of its impulse response matrix $\mathbf{h}(t)$ are vanishing for $t < 0$, i.e.,

$$\mathbf{h}(t) = 0, \quad t < 0. \qquad (2)$$

Proof: For the sake of simplicity, we consider a scalar impulse response $h(t)$. Condition (2) is necessary for causality because if a Dirac's delta $\delta(t)$ is taken as input, the output is $w(t) = h(t) * \delta(t) = h(t)$. Since input vanishes for $t < 0$, then, for Theorem III.1, the output $h(t)$ must vanish too for $t < 0$.

Condition (2) is also sufficient to guarantee causality. In this case (1) becomes

$$w(t) = \int_{-\infty}^{t} h(t-\tau)x(\tau)\, d\tau$$

and, due to the upper integration limit, causality follows from Theorem III.1. ■

Remark III.1: The above definitions of causality are general and apply to both lumped and distributed systems. In the latter case, however, it may be important to adopt a more stringent definition by explicitly considering the propagation delays due to the finite propagation speed of signals [33]

$$h_{ij}(t) = 0, \quad t < T_{ij}, \quad T_{ij} \ge 0 \quad \forall i, j.$$

This holds, e.g., in any transmission-line network. The identification of models that take into account these propagation delays is indeed an active research area [15]–[24]. Throughout this paper, we will adopt the delay-free definition of causality of Theorem II.2. Therefore, we will always refer to *causality* meaning zero-delay causality.

B. Stability

The concept of stability is related to the boundedness of the system responses. In fact, engineers always verify that their circuits are stable in order to be sure that no inputs can drive them beyond operating limits. For this reason, although several different definitions of stability are available, herewith we consider the so-called bounded-input bounded-output (BIBO) definition of stability [28].

Definition III.2 (Stability): A system is stable if the output $\mathbf{w}(t)$ is bounded[3] for all bounded inputs $\mathbf{x}(t)$.

The BIBO stability is guaranteed in an LTI system if and only if all elements of $\mathbf{h}(t)$ are such that

$$\int_{-\infty}^{+\infty} |h_{ij}(t)|\, dt < +\infty. \qquad (3)$$

[3]A vector $\mathbf{w}(t)$ is bounded if any of its components $w_i(t)$ is such that $|w_i(t)| < M, \forall t$.

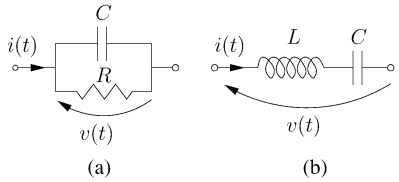

Fig. 3. Circuits for Examples III.1 and III.2.

The above condition applies to both lumped and distributed systems.

Example III.1: Let us consider a physical realization of an RC circuit, as shown in Fig. 3(a). Since this circuit is made of real components, causality should be assumed *a priori*. Under this hypothesis, the impedance impulse response is

$$h(t) = Ae^{pt}u(t), \quad p = -\frac{1}{RC}, \quad A = \frac{1}{C} \tag{4}$$

where $u(t)$ denotes the unit step (Heaviside) function. Stability depends on the sign of R and C. If both are positive (as is true for real resistors and capacitors), then $p < 0$, the integral in (3) is bounded, and the system turns out to be BIBO stable. Conversely, if for example R is negative (as can be obtained by employing an active device, at least within a given voltage range), $h(t)$ grows for large t, and stability does not hold.

Example III.2: We consider the physical circuit shown in Fig. 3(b). The impulse response in the admittance representation is

$$h(t) = A\cos(\omega_0 t)u(t), \quad \omega_0 = \frac{1}{\sqrt{LC}}, \quad A = \frac{1}{L} \tag{5}$$

and violates (3). The system is thus not BIBO stable. This is further confirmed by choosing the bounded input $x(t) = \sin(\omega_0 t)u(t)$, which produces the unbounded output $w(t) = (t/2L)\sin(\omega_0 t)u(t)$. This is the well-known principle of (lossless) resonance, which will be discussed in more detail in Section IV.

C. Passivity

A physical system is denoted as passive when it is unable to generate energy. The precise mathematical definition of passivity depends on the representation adopted for the n-port network. For impedance or admittance representations we have [27].

Definition III.3 (Passivity): An n-port network is said to be passive if

$$\int_{-\infty}^{t} \mathbf{v}^T(\tau)\mathbf{i}(\tau)\,d\tau \geq 0 \tag{6}$$

for *all* t and *all* admissible port voltages $\mathbf{v}(t)$ and currents $\mathbf{i}(t)$.

For scattering representations, the passivity definition is similar, with (6) replaced by

$$\int_{-\infty}^{t} [\mathbf{a}^T(\tau)\mathbf{a}(\tau) - \mathbf{b}^T(\tau)\mathbf{b}(\tau)]\,d\tau \geq 0 \tag{7}$$

where $\mathbf{a}(t)$ and $\mathbf{b}(t)$ are, respectively, the incident and reflected power waves at the ports. The above definitions apply to both lumped and distributed systems.

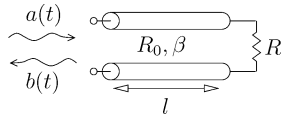

Fig. 4. Circuit considered in Example III.3.

Integrals in (6) and (7) represent the cumulative net energy absorbed by the system up to instant t. This energy has to be positive for all t in any passive system. This requirement is satisfied if two conditions hold: 1) the system absorbs more energy than it generates and 2) the possible generation occurs *after* absorption. A noncausal system that first generates energy and then absorbs it, even to a larger extent, is thus considered nonpassive. With this consideration in mind, it is not surprising that all passive systems are causal [27], [26].

Theorem III.3: If an LTI system is passive, then it is also causal.

Proof: We prove this important result for the scattering representation; a similar result holds for the impedance/admittance representations [27]. For simplicity, we focus on a one-port system with input $a(t)$ and output $b(t)$. The proof establishes causality by verifying that, for passive systems, Theorem III.1 always holds. We choose an arbitrary input signal $a(t)$ that vanishes for $t < t_0$. The passivity definition (7) requires that

$$\int_{-\infty}^{t} b^2(\tau)\,d\tau \leq 0, \quad t < t_0.$$

The integrand function is non-negative by construction. Therefore, the above inequality holds for all $t < t_0$ only if the output $b(t)$ vanishes for $t < t_0$. Hence, the system is causal. ■

Example III.3: Fig. 4 depicts an ideal transmission line (characteristic impedance R_0, propagation constant β, length l) terminated by a load resistor R. If R_0 is assumed as the reference port impedance, the reflected power wave $b(t)$ turns out to be

$$b(t) = \Gamma_R a(t - 2t_0), \quad \Gamma_R = \frac{R - R_0}{R + R_0} \tag{8}$$

where $t_0 = \beta l$ is the one-way time-of-flight of the line. Obviously, this system is passive if R is positive. We prove this by applying the passivity condition (7), which in this case becomes

$$\int_{-\infty}^{t} \left[a^2(\tau) - \Gamma_R^2 a^2(\tau - 2t_0)\right] d\tau = \left(1 - \Gamma_R^2\right) \int_{-\infty}^{t-2t_0} a^2(\tau)\,d\tau + \int_{t-2t_0}^{t} a^2(\tau)\,d\tau \geq 0.$$

In the above inequality, both integrals are positive for any possible input signal $a(t)$. Therefore, the sign of the entire expression depends only on the factor $(1 - \Gamma_R^2)$ that is positive if

$$|\Gamma_R| = \left|\frac{R - R_0}{R + R_0}\right| \leq 1 \Leftrightarrow R \geq 0.$$

So, if $R \geq 0$, (7) holds and the system is passive as expected.

Remark III.2: Theorem III.3 has two important consequences. First, since all passive systems are causal, any noncausal system cannot be passive. Second, any macromodeling algorithm that enforces model passivity will also guarantee

model causality. Conversely, a model that violates causality will violate passivity too, as pointed out in the next example.

Example III.4: We consider again the structure of Example III.3, but with a negative delay, i.e., $t_0 < 0$. This system is clearly noncausal, since the output $b(t) = \Gamma_R a(t-2t_0)$ is an anticipated version of the input $a(t)$. Of course, a physical equivalent does not exist. However, it is an interesting illustration of the fact that noncausal systems are also nonpassive. We show the lack of passivity by noting that the passivity condition (7), for an input $a(\tau)$ that vanishes for $\tau \in (-\infty, t]$, reads

$$-\Gamma_R^2 \int_t^{t-2t_0} a^2(\tau)\, d\tau \geq 0.$$

This condition is never satisfied because of the negative sign in front of the certainly positive integral. This example also shows that any passivity violation can be highlighted or detected by choosing an appropriate input that results in a negative absorbed energy.

IV. Laplace Domain

The Laplace transform is the natural tool for the analysis of LTI systems, since it transforms differential time-domain operators into algebraic s-domain operators. In Laplace domain, (1) becomes

$$\mathbf{W}(s) = \mathbf{H}(s)\mathbf{X}(s) \tag{9}$$

where $\mathbf{H}(s)$ represents the system transfer function.

In this section, we derive the conditions for stability, causality, and passivity in the Laplace domain. However, we should be careful in using the appropriate definition of the transform. In fact, the widely used unilateral Laplace transform, defined as

$$\mathsf{L}\{f(t)\} = \int_0^{+\infty} f(t)e^{-st}\, dt \tag{10}$$

is not appropriate for our analysis, since it neglects by construction any part of the signal for $t < 0$. All signals are automatically treated as causal, hence no conditions for causality can be inferred if definition (10) is used. If we want to derive suitable conditions for causal systems, it is necessary to extend the time integration down to $-\infty$, by using the bilateral Laplace transform.

A. Bilateral Laplace Transform

The bilateral Laplace transform is defined as [28]

$$F(s) = \mathsf{L}_b\{f(t)\} = \int_{-\infty}^{+\infty} f(t)e^{-st}\, dt \tag{11}$$

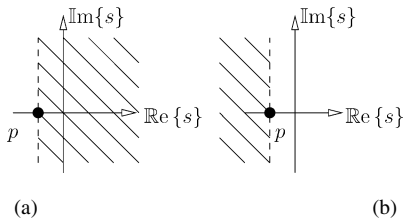

Fig. 5. ROC of bilateral Laplace transforms (a) $\mathsf{L}_b\{f_1(t)\}$ and (b) $\mathsf{L}_b\{f_2(t)\}$ as in Example IV.1.

where $s = \sigma + j\omega$. The key difference[4] between bilateral and unilateral Laplace transform is the importance of the region of convergence (ROC), i.e., the set of s values for which the integral in (11) converges absolutely. We illustrate this via a simple example.

Example IV.1: Consider the two distinct functions $f_1(t) = e^{pt}u(t)$ and $f_2(t) = -e^{pt}u(-t)$, where p is a real quantity. A direct calculation from (11) leads to

$$\mathsf{L}_b\{f_1(t)\} = F_1(s) = \frac{1}{s-p}, \quad \text{ROC: } \mathbb{R}\mathrm{e}\{s\} > p \tag{12}$$

$$\mathsf{L}_b\{f_2(t)\} = F_2(s) = \frac{1}{s-p}, \quad \text{ROC: } \mathbb{R}\mathrm{e}\{s\} < p \tag{13}$$

so that the actual transformed functions take identical expressions. Therefore, the only way to discriminate them is the knowledge of their respective ROCs, depicted in Fig. 5.

We will show that the ROC plays a fundamental role for the characterization of both causality (f_1 is causal and f_2 is not) and stability. For completeness, we report four general ROC properties, clearly verified for the above example.

1) ROC is always, in the complex $s = \sigma + j\omega$ plane, a strip parallel to the imaginary axis.
2) If a function $f(t)$ vanishes for $t < t_0$, its ROC is a half-plane open on the right, i.e., $\mathbb{R}\mathrm{e}\{s\} > \sigma_0$ for some σ_0.
3) $F(s)$ is analytic[5] inside its ROC.
4) ROC is bounded on its left and right by the singularities of $F(s)$ (poles for lumped systems).

Although inversion of (11) can be computed via line integration within the ROC [28], inverse Laplace transform is usually obtained (at least for lumped systems) by partial fractions decomposition, as shown in the following example.

Example VI.2: The function $F(s) = 1/((s+1)(s+2))$ with ROC $-2 < \mathbb{R}\mathrm{e}\{s\} < -1$ is decomposed as

$$\frac{1}{(s+1)(s+2)} = \underbrace{\frac{1}{s+1}}_{\mathbb{R}\mathrm{e}\{s\}<-1} - \underbrace{\frac{1}{s+2}}_{\mathbb{R}\mathrm{e}\{s\}>-2}. \tag{14}$$

The regions of convergence of the two partial fractions have to be chosen such that their intersection is the ROC of $F(s)$. According to the above-mentioned properties, the possible ROCs for the first term $(1)/(s+1)$ are $\mathbb{R}\mathrm{e}\{s\} < -1$ and $\mathbb{R}\mathrm{e}\{s\} > -1$ and, for the second one, are $\mathbb{R}\mathrm{e}\{s\} < -2$ and $\mathbb{R}\mathrm{e}\{s\} > -2$.

[4]Bilateral Laplace transform (11) has the same properties of the unilateral one [28], except for the transform of a differentiated signal, which turns out to be $\mathsf{L}_n\{(d/dt)f(t)\} = sF(s)$.

[5]A function $F(s)$ of a complex variable s is analytic in a region Ω if it has no poles nor other singularities (e.g., branch points) in Ω.

The individual ROCs reported in (14) are the only combination which is compatible with the ROC of the original function. The inverse Laplace transform is then $f(t) = -e^{-t}u(-t) - e^{-2t}u(t)$.

B. Causality

In a causal system, since each element of $\mathbf{h}(t)$ is vanishing for negative time, the ROC for each of the elements of $\mathbf{H}(s)$ is a half-plane open on the right. However, this condition is not sufficient for causality. The following theorem [29] provides a precise characterization.

Theorem IV.1: A signal $h(t)$ is vanishing for $t < 0$ if and only if its bilateral Laplace transform:

1) is defined and analytic in a half-plane $\mathbb{R}\mathrm{e}\{s\} > \sigma_0$;
2) grows not faster than a polynomial for $\mathbb{R}\mathrm{e}\{s\} > \sigma_0$.

The importance of the two conditions stated by this theorem is highlighted by the following two examples.

Example VI.3: The Laplace transforms $F_1(s)$ and $F_2(s)$ of Example VI.1 clearly show that a ROC open on the right is necessary for causality. The first function is defined for $\mathbb{R}\mathrm{e}\{s\} > p$ and is associated to a time-domain signal $f_1(t) = e^{pt}u(t)$ that vanishes for $t < 0$. Conversely, $F_2(s)$, in spite of sharing the same mathematical expression of $F_1(s)$, is defined in a completely different ROC and does not satisfy the conditions stated by Theorem IV.1. Its inverse Laplace transform $f_2(t) = -e^{pt}u(-t)$ is thus a noncausal signal.

Example IV.4: The scattering matrix of the circuit in Fig. 4 is

$$S(s) = \Gamma_R e^{-2st_0}, \quad \Gamma_R = \frac{R - R_0}{R + R_0} \tag{15}$$

and is defined and analytic over the entire complex s plane. Consequently, it satisfies the first condition stated in Theorem IV.1 whatever t_0 is; however, $S(s)$ is causal only if $t_0 \geq 0$, requiring that the exponential factor represents a true delay and not a noncausal anticipation. In the latter case with $t_0 < 0$, the second condition of Theorem IV.1 is obviously violated since $S(s)$ grows exponentially for $\mathbb{R}\mathrm{e}\{s\} > 0$.

C. Stability

The ROC associated to a system transfer function is important to ascertain stability. We have the following theorem (for lumped systems).

Theorem IV.2: A system is stable according to Definition III.2 if and only if: 1) the ROC associated to its transfer matrix $\mathbf{H}(s)$ includes the imaginary axis and 2) $\mathbf{H}(\infty)$ is bounded.

This condition is quite different from the more practical rule normally employed by engineers, who usually test stability by checking that all the system poles have negative real part. For causal systems, both criteria are equivalent. In fact, since the ROC for any causal system is open on the right and is bounded on the left by the system singularities, when these singularities are confined to the left-hand plane, the ROC will necessarily include the imaginary axis, as shown in Fig. 6. For noncausal systems, however, only the analysis of the region of convergence allows us to prove stability, as shown in the next example.

Theorem III.1: Consider the impulse responses

$$h_1(t) = e^{pt}u(t) \quad H_1(s) = \frac{1}{s-p}, \quad \text{ROC: } \mathbb{R}\mathrm{e}\{s\} > p$$

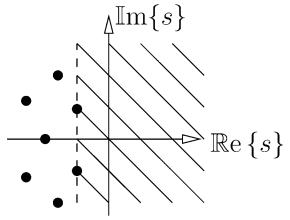

Fig. 6. When a causal transfer function has all singularities confined in left-hand plane, ROC surely includes imaginary axis.

$$h_2(t) = -e^{pt}u(-t) \quad H_2(s) = \frac{1}{s-p}, \quad \text{ROC: } \mathbb{R}\mathrm{e}\{s\} < p.$$

As already discussed in Example III.1, $h_1(t)$ is stable only if $p < 0$, in which case the ROC includes the imaginary axis. Since $h_1(t)$ is causal, the stability condition is thus equivalent to requiring that the system pole lies in left hand plane. When $p > 0$, the ROC does not include the imaginary axis and $h_1(t)$ is unstable. We have a different situation for the noncausal impulse response $h_2(t)$, which is stable when $p > 0$, i.e., when its ROC includes the imaginary axis.

Example IV.6: The admittance of the LC resonator depicted in Fig. 3(b) is

$$Y(s) = \frac{1}{L}\frac{s}{s^2 + \frac{1}{LC}} \quad \text{ROC: } \mathbb{R}\mathrm{e}\{s\} > 0 \tag{16}$$

where the ROC has been chosen open on the right in order to insure causality. In this case, the ROC does not include the imaginary axis, where the two system poles $s = \pm j/\sqrt{LC}$ are located. Therefore, according to Theorem IV.2, the system is not BIBO stable, as reported also in Example III.2. This example confirms that systems with purely imaginary poles are a boundary case for stability, and the adopted definition of BIBO stability rules out these systems. Under a practical standpoint, we believe that this definition satisfies the theoretical need of a design engineer, since lossless resonant structures never occur in practice due to the unavoidable presence of losses. In addition, any model which has poles on the imaginary axis may become critical under certain excitations and should be carefully avoided.

D. Passivity

The passivity conditions in Laplace domain depend on the adopted representation. In the impedance or admittance cases we have [26].

Theorem IV.3: An impedance matrix $\mathbf{Z}(s)$ represents a passive linear system if and only if:

1) each element of $\mathbf{Z}(s)$ is defined and analytic in $\mathbb{R}\mathrm{e}\{s\} > 0$;
2) $\mathbf{Z}^H(s) + \mathbf{Z}(s)$ is a nonnegative-definite matrix[6] for all s such that $\mathbb{R}\mathrm{e}\{s\} > 0$;
3) $\mathbf{Z}(s^*) = \mathbf{Z}^*(s)$.

The superscripts * and ^{H} denote the complex conjugate and transpose conjugate, respectively. Note that the second condition generalizes for the matrix case the requirement that a passive one-port impedance must have positive real part. The third condition ensures that the associated impulse response is real.

[6]A complex Hermitian matrix $\mathbf{A} = \mathbf{A}^H$ is nonnegative-definite if $\mathbf{x}^H\mathbf{A}\mathbf{x} \geq 0$ for all complex vectors $\mathbf{x} \neq 0$.

The first condition is related to causality and stability, since it requires a ROC that is open on the right and touching the imaginary axis. In fact, it is possible to prove that the three above conditions for passivity always imply causality. The first condition also implies BIBO stability, provided that the system has no singularities on the imaginary axis (i.e., purely imaginary poles).

Remark IV.1: From the above discussion, it appears evident that passivity is the strongest requirement for the well-posedness and physical consistency of a given model, since passivity implies both causality and stability.

Example IV.7: The impedance of the RC circuit shown in Fig. 3(a) (with positive R and C) is

$$Z(s) = \frac{1}{C}\frac{1}{s+\frac{1}{RC}} \quad \text{ROC: } \mathbb{R}\mathrm{e}\{s\} > -\frac{1}{RC} \tag{17}$$

and clearly satisfies the first and third conditions reported in Theorem IV.3. The second condition reads

$$Z(s) + Z^H(s) = \frac{2}{C}\frac{\sigma+\frac{1}{RC}}{|s+\frac{1}{RC}|^2} \geq 0$$

where $s = \sigma + j\omega$ and is satisfied because, for $\mathbb{R}\mathrm{e}\{s\} = \sigma > 0$, all quantities are positive.

Example IV.8: A similar calculation proves that the admittance function (16) of the LC resonator in Fig. 3(b) is passive. In fact, the second condition of Theorem IV.3 becomes

$$Y(s) + Y^H(s) = \frac{2}{L}\frac{\sigma(\sigma^2+\omega^2+\frac{1}{LC})}{|s^2+\frac{1}{LC}|^2} \geq 0$$

and is satisfied for $\mathbb{R}\mathrm{e}\{s\} = \sigma > 0$.

For the scattering representation we have a similar result [26].

Theorem IV.4: A scattering matrix $\mathbf{S}(s)$ represents a passive linear system if and only if:

1) each element of $\mathbf{S}(s)$ is analytic in $\mathbb{R}\mathrm{e}\{s\} > 0$;
2) $\mathbf{I} - \mathbf{S}^H(s)\mathbf{S}(s)$ is a nonnegative-definite matrix for all s such that $\mathbb{R}\mathrm{e}\{s\} > 0$;
3) $\mathbf{S}(s^*) = \mathbf{S}^*(s)$.

A matrix fulfilling these three conditions is said to be bounded real. Conditions 1) and 3) have the same meaning as in Theorem IV.3. Condition 2) is basically a bound for $\mathbf{S}(s)$, which generalizes the basic condition on passive one-port networks having a reflection coefficient not larger than one. An alternative and equivalent condition requires that $||\mathbf{S}(s)||_2$, i.e., the largest singular value of $\mathbf{S}(s)$, does not exceed one in the right-hand plane.

Example IV.9: The scattering coefficient (15) of the circuit depicted in Fig. 4 satisfies the passivity constraints only if $R > 0$. In fact, conditions 1) and 3) of Theorem IV.4 hold independently of R, while condition 2) holds only if $R > 0$, since it requires that

$$|\Gamma_R|^2 e^{-4t_0\sigma} \leq 1$$

for all $\sigma > 0$. If R is negative, then $|\Gamma_R| > 1$ and the above inequality does not hold for small values of σ.

V. Frequency Domain

The Laplace-domain conditions reviewed in Section IV are exhaustive but may be difficult to check, since they require testing the entire or at least half of the complex s-plane. However, these results may be restricted to the imaginary axis $s = j\omega$ only, by considering the standard Fourier transform

$$F(j\omega) = \mathsf{F}\{f(t)\} = \int_{-\infty}^{+\infty} f(t)e^{-j\omega t}\,dt \tag{18}$$

instead of the Laplace transform. Of course, use of Fourier transform makes sense only if the integral (18) exists (converges). The resulting frequency-domain equivalent of (1) is

$$\mathbf{W}(j\omega) = \mathbf{H}(j\omega)\mathbf{X}(j\omega) \tag{19}$$

and makes sense only when the Fourier transform exists for both the system impulse response $\mathbf{h}(t)$ and the excitation signal $\mathbf{x}(t)$. It is well known that $\mathbf{H}(j\omega)$ is directly related to the sinusoidal steady-state response and it can be directly measured.

A. Stability

Fourier analysis is always possible for stable systems, because if (3) is satisfied, the integral in (18) converges absolutely. Difficulties arise for unstable systems, as shown in the following example.

Example V.1: The frequency-domain impedance representation of the circuit in Fig. 3(a) is

$$Z(j\omega) = A\frac{1}{j\omega - p}, \quad p = -\frac{1}{RC}, \quad A = \frac{1}{C} \tag{20}$$

and exists *only* if $p < 0$. In fact, the system impulse response is $Ae^{pt}u(t)$ and cannot be Fourier transformed via (18) if $p > 0$, consistent with the fact that a sinusoidal steady state is never established in such an unstable system.

For unstable systems, the Laplace transform is a more appropriate tool, since it can be defined regardless of stability, as discussed in Section IV. Bilateral Laplace and Fourier transforms can both be defined if the ROC includes the imaginary axis.

B. Causality

Causality imposes strong conditions on the frequency response of a system. Denoting as $h(t)$ a causal impulse response (vanishing for $t < 0$), we have

$$h(t) = \mathrm{sign}(t)h(t)$$

where $\mathrm{sign}(t)$ is the sign function that equals 1 for $t > 0$ and -1 for $t < 0$. Applying Fourier transform[7] one obtains

$$\mathsf{F}\{h(t)\} = \frac{1}{2\pi}\mathsf{F}\{\mathrm{sign}(t)\} * \mathsf{F}\{h(t)\}$$

since the transform of the product $\mathrm{sign}(t)h(t)$ leads to a convolution. A direct calculation leads to

$$H(j\omega) = \frac{1}{j\pi}\ \mathrm{pv}\int_{-\infty}^{+\infty}\frac{H(j\omega')}{\omega-\omega'}\,d\omega' \tag{21}$$

where the integral converges despite of the integrand singularity for $\omega' = \omega$, because the principal value

$$\mathrm{pv}\int_{-\infty}^{+\infty} = \lim_{\epsilon\to 0^+}\left[\int_{-\infty}^{\omega-\epsilon} + \int_{\omega+\epsilon}^{+\infty}\right] \tag{22}$$

[7]Mathematically, this calculation has to be done with distributions.

is taken. In order to appreciate the strong implications of (21), it is useful to divide it into real and imaginary parts

$$U(\omega) = \frac{1}{\pi}\,\mathrm{pv}\int_{-\infty}^{+\infty}\frac{V(\omega')}{\omega-\omega'}\,d\omega' \tag{23a}$$

$$V(\omega) = -\frac{1}{\pi}\,\mathrm{pv}\int_{-\infty}^{+\infty}\frac{U(\omega')}{\omega-\omega'}\,d\omega' \tag{23b}$$

where $H(j\omega) = U(\omega) + jV(\omega)$. These equations, known as Kramers–Krönig dispersion relations [31]–[34], are valid for every causal system and state that the frequency response real and imaginary parts are not independent. Kramers–Krönig relations are necessary and also sufficient for causality, as stated by the next theorem.

Theorem V.1: If $h(t)$ admits a Fourier transform, the following facts are equivalent.

1) $h(t) = 0$ for $t < 0$;
2) $H(j\omega)$ is the limit, as $\sigma \to 0$, of a function $H(s)$ defined in $\mathbb{R}\mathrm{e}\{s\} > 0$ and here analytic and of polynomial growth;
3) $H(j\omega) = \mathsf{F}\{h(t)\}$ satisfies Kramers–Krönig relations.

This interesting result, due to Titchmarsh [34] and generalized by Beltrami [30], summarizes and relates the conditions for causality in time, Laplace, and frequency domains.

Example V.2: We consider the frequency response

$$H(j\omega) = \frac{1}{j\omega - p} = \underbrace{\frac{-p}{\omega^2+p^2}}_{U(\omega)} + j\,\underbrace{\frac{-\omega}{\omega^2+p^2}}_{V(\omega)} \tag{24}$$

with $p \in \mathbb{R}$ and test whether its real part $U(\omega)$ and imaginary part $V(\omega)$ satisfy dispersion relations. The integral in (23a) can be computed by using the following decomposition into partial fractions:

$$\frac{-\omega'}{\omega'^2+p^2}\frac{1}{\omega-\omega'} = \frac{-\omega}{\omega^2+p^2}\frac{1}{\omega-\omega'} - \frac{\omega}{\omega^2+p^2}\frac{\omega'}{\omega'^2+p^2} + \frac{p^2}{\omega^2+p^2}\frac{1}{\omega'^2+p^2}.$$

This allows us to write

$$\mathrm{pv}\int_{-\infty}^{+\infty}\frac{-\omega'}{\omega'^2+p^2}\frac{d\omega'}{\omega-\omega'} = \frac{p^2}{\omega^2+p^2}\,\mathrm{pv}\int_{-\infty}^{+\infty}\frac{d\omega'}{\omega'^2+p^2}$$

since the first two partial fraction terms above are odd-symmetric, thus leading to a vanishing principal value integral. Finally, we have

$$\frac{1}{\pi}\,\mathrm{pv}\int_{-\infty}^{+\infty}\frac{V(\omega')}{\omega-\omega'}\,d\omega' = \frac{|p|}{p^2+\omega^2}. \tag{25}$$

This computed real part matches (24), i.e., the system is causal according to (23a), only if $p < 0$. Of course, this is consistent with the fact that the extension of $H(j\omega)$ to a Laplace transform in the complex s-plane reads

$$H(s) = \frac{1}{s-p} \quad \text{ROC: } \mathbb{R}\mathrm{e}\{s\} > p, \quad p < 0$$

because the ROC must include the imaginary axis where the original frequency response is defined. Conversely, if $p > 0$ the frequency response is noncausal since:

1) dispersion relations are not satisfied;
2) the extension of $H(j\omega)$ to a Laplace transform in the complex s-plane reads

$$H(s) = \frac{1}{s-p} \quad \text{ROC: } \mathbb{R}\mathrm{e}\{s\} < p, \quad p > 0$$

and the ROC is not a half-plane open on the right;
3) the associated time-domain signal is $h(t) = -e^{pt}u(-t)$, which is obviously noncausal.

C. Passivity

The Laplace-domain passivity conditions stated by Theorems IV.3 and IV.4 have to be verified in the entire half-plane $\mathbb{R}\mathrm{e}\{s\} > 0$. We report here some passivity conditions that practically require testing only the imaginary axis $s = j\omega$.

The following theorem [26] applies only to lumped systems, whose transfer functions are always rational.

Theorem V.2: A rational matrix $\mathbf{Z}(s)$ is the impedance of a passive lumped system if and only if:

1) each element of $\mathbf{Z}(s)$ is defined and analytic in $\mathbb{R}\mathrm{e}\{s\} > 0$;
2) $\mathbf{Z}^H(j\omega) + \mathbf{Z}(j\omega)$ is a nonnegative-definite matrix for all $\omega \in \mathbb{R}$, except for simple poles $j\omega_0$ of $\mathbf{Z}(s)$, where the residue matrix must be nonnegative definite;
3) $\mathbf{Z}(-j\omega) = \mathbf{Z}^*(j\omega)$;
4) asymptotically, $\mathbf{Z}(s) \to \mathbf{A}s$ in $\mathbb{R}\mathrm{e}\{s\} > 0$, where $\mathbf{A}$ is a real, constant, symmetric, nonnegative-definite matrix.

A similar result holds for the admittance matrix $\mathbf{Y}(s)$.

Example V.3: The impedance of the circuit depicted in Fig. 3(b) is

$$Z(s) = sL + \frac{1}{sC} \quad \text{ROC: } \mathbb{R}\mathrm{e}\{s\} > 0. \tag{26}$$

This is a rational function, so we can apply Theorem V.2 to ascertain passivity. The first condition of the theorem is satisfied because $Z(s)$ is analytic in the whole complex plane except for $s = 0$; condition 2) holds because for $s = j\omega$ one has $Z^H(j\omega) + Z(j\omega) = 0$. Condition 3) is satisfied as well as condition 4), since asymptotically $Z(s) \to sL$.

The corresponding result of Theorem V.2 for the scattering representation (valid for both lumped and distributed systems) reads as follows [26].

Theorem V.3: A scattering matrix $\mathbf{S}(j\omega)$ represents a passive linear system if and only if:

1) dispersion relations (23) hold;
2) $\mathbf{I} - \mathbf{S}^H(j\omega)\mathbf{S}(j\omega)$ is a nonnegative-definite matrix for all ω;
3) $\mathbf{S}(-j\omega) = \mathbf{S}^*(j\omega)$.

Note that this theorem involves only conditions restricted to the imaginary axis $s = j\omega$. It is remarkable that the combined conditions 1) (dispersion relations) and 2) (unitary boundedness) are sufficient to control the function behavior in $\mathbb{R}\mathrm{e}\{s\} > 0$, i.e., passivity. Therefore, it appears that the scattering representation is more appealing for practical use in data and model verification. Of course, if $\mathbf{S}(s)$ is rational and analytic in $\mathbb{R}\mathrm{e}\{s\} > 0$, only conditions 2) and 3) are necessary, since dispersion relations are automatically satisfied.

Example V.4: The second condition of Theorem V.3, written for the scattering parameter of the circuit in Fig. 4

$$S(j\omega) = \Gamma_R e^{-2j\omega t_0} \quad \Gamma_R = \frac{R - R_0}{R + R_0} \tag{27}$$

reads

$$\begin{aligned} \mathbf{I} - \mathbf{S}^H(j\omega)\mathbf{S}(j\omega) &= 1 - \Gamma_R^2 e^{2j\omega t_0} e^{-2j\omega t_0} \\ &= 1 - \Gamma_R^2 \geq 0. \end{aligned}$$

When $|\Gamma_R| \leq 1$ this inequality is always satisfied, independently of t_0. However, if $t_0 < 0$ the system is not causal (as discussed in Example III.4) and hence nonpassive. This example points out that condition 2) (unitary boundedness) is not sufficient to ascertain the passivity of distributed systems. It is necessary, as stated by Theorem V.3, to also ensure that dispersion relations are satisfied, i.e., that the system is causal.

VI. Examples

A. Analytic Example

We start with a simple analytic example. Despite its apparent triviality, this example is quite significant since it allows us to pinpoint via analytic derivations a typical source of problems in real-life modeling and simulation tasks. We consider the scattering frequency response

$$S(j\omega) = \frac{1}{1 + \omega^2} \tag{28}$$

and we want to derive an equivalent model that can be used in a time-domain simulation tool.

1) Causal and Unstable Model: The typical approach for macromodel derivation is to fit the data with a rational expression in the Laplace domain. In this case, an error-free fit is possible and leads to the expression

$$S(s) = \frac{1}{1 - s^2}. \tag{29}$$

In fact, (29) reduces exactly to (28) when evaluated for $s = j\omega$. The model poles are $p = \pm 1$, with one unstable pole with positive real part. The corresponding impulse response is exponentially unstable. Fig. 7 provides a further illustration of this instability by depicting (continuous line) the results of a computer simulation of the model (29) when a square pulse is applied as input. It is clear that any practical use of this model is impossible, even if the match to the data is perfect.

2) Stable and Noncausal Model: An alternative approach to compute the time-domain response of (28) under a given excitation $x(t)$ is via inverse Fourier transform

$$w(t) = \mathsf{F}^{-1}\{S(j\omega)X(j\omega)\}, \quad X(j\omega) = \mathsf{F}\{x(t)\}. \tag{30}$$

The result for a square pulse input is depicted with a dashed line in Fig. 7. It is clear that the model is not causal, but stable. Also in this case, if proper care is taken in computing the inverse Fourier transform, the computed response is virtually error free.

3) Discussion: It appears that two models with very different behavior and characterized by different fundamental properties are compatible with (28). The main reason for this inconsistency is the lack of causality of the original data (28). In fact, this frequency response is not causal because it violates Theorem V.1, whatever condition is considered.

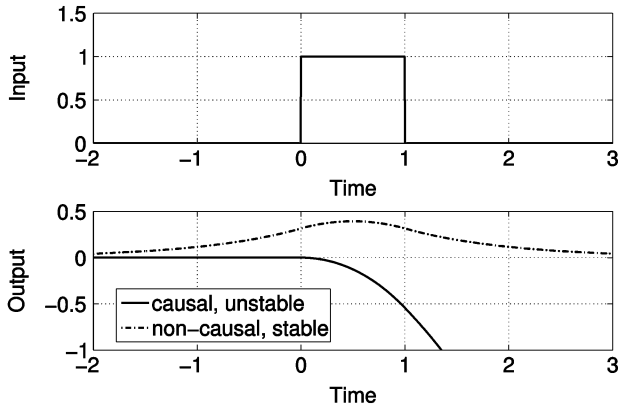

Fig. 7. Response of two different time-domain models of (28) to a square pulse. Continuous line refers to (29), and dashed line is obtained via inverse Fourier transform.

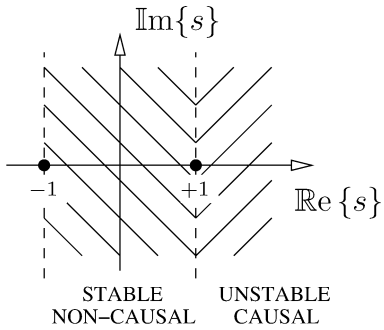

Fig. 8. Graphical illustration of ROC for two models of Section IV-A.

1) The inverse Fourier transform of (28) is

$$s(t) = \mathsf{F}^{-1}\{S(j\omega)\} = \frac{1}{2}e^{-|t|}$$

which does not vanish for $t < 0$.

2) The extension of $S(j\omega)$ to the entire s-plane,

$$S(s) = \frac{1}{1 - s^2} \quad \text{ROC: } -1 < \mathbb{R}\mathrm{e}\{s\} < 1$$

is not defined in the half-hand plane $\mathbb{R}\mathrm{e}\{s\} > 0$ (note that the ROC has to be defined so that it includes the imaginary axis).

3) The frequency response itself does not satisfy the dispersion relations (23). In fact, a straightforward calculation (as in Example V.2) reveals that $S(j\omega)$ requires an associated imaginary part $-\omega/(1 + \omega^2)$ in order to be causal.

A clear picture of the situation is provided by Fig. 8. Each of the two models is characterized by a different ROC, and we know from Section IV that the ROC determines directly the stability and the causality properties of the model. Due to the singularity at $s = 1$, a simultaneous enforcement of stability and causality is not possible.

In summary, given a noncausal dataset as in (28), the objective of computing a causal and stable model becomes an ill-posed problem. It is of course possible to compute a rational approximation by constraining all poles to be stable, so that the ROC

TABLE III
FAILURE OF A CAUSAL AND STABLE RATIONAL MODEL FIT TO NONCAUSAL DATASET OF SECTION VI-A

Model order	Maximum error
4	0.523
8	0.416
12	0.417
16	0.422
20	0.422

will be open on the right and include the imaginary axis. Unfortunately, such a fit will be very poor and the accuracy will not be under control. Table III reports the results of VF applied to this example, with a varying number of (strictly stable) poles. It is clear that the approximation does not converge to the data, as expected.

We conclude this example with a remark. Most time-domain circuit solvers adopt a forward time-stepping procedure to compute the solution. In this framework, it is implicitly assumed that the solution at a given time iteration is only influenced by the previous and already computed times, which is essentially the same requirement of causality. Hence, causality is a must for each model in the network. Equivalently, noncausal models are not compatible with time-stepping solvers. In addition, even the concept of initial conditions (required for setting up the time iterations) may become meaningless or difficult to apply when causality is not assumed *a priori*.

B. Revisiting Test Case of Section II

We reconsider now the example reported in Section II, for which an accurate rational fit with stable poles only was not possible. This is actually the same scenario that was encountered in the simple example of Section VI-A. We may argue that the main reason is hidden in some causality violations of the raw frequency response. However, in this case only a set of tabulated frequency points are available, and no analytic expressions will help us in the verification of this hypothesis. This is the practical situation that a design engineer would actually face with no source of information available other than the results of his measurement or field simulation.

Among the various conditions for testing causality that were reviewed in this paper, it appears that the direct application of the dispersion relations (23) is the only feasible option in this case. Due to the singular nature of the integrals and to the availability of samples over a limited frequency band, the direct computation of (23) may be very inaccurate. This problem has been addressed in [40] and [41], where an accurate and robust methodology to ascertain the causality of tabulated frequency responses is developed, based on a generalized form of the Hilbert transform. We applied this method to the available frequency data, and the results are shown in Figs. 9 and 10. The solid lines represent the original data, while the gray shaded areas are frequency-dependent regions where the data should lay in order to satisfy causality (details can be found in [40]). When a data point is outside these areas we are sure that a causality violation is present.

These results confirm that the failure reported in Section II is really due to causality violations in the data. However, the detection of such violations requires a sophisticated numerical tool. This example should illustrate how critical it may be to handle a flawed dataset. The symptoms of data inconsistencies only appear when trying to build a macromodel, and it may not be clear to the engineer what is the real cause of the problems. It is also evident that any dataset should be certified for causality before attempting any macromodeling and simulation step.

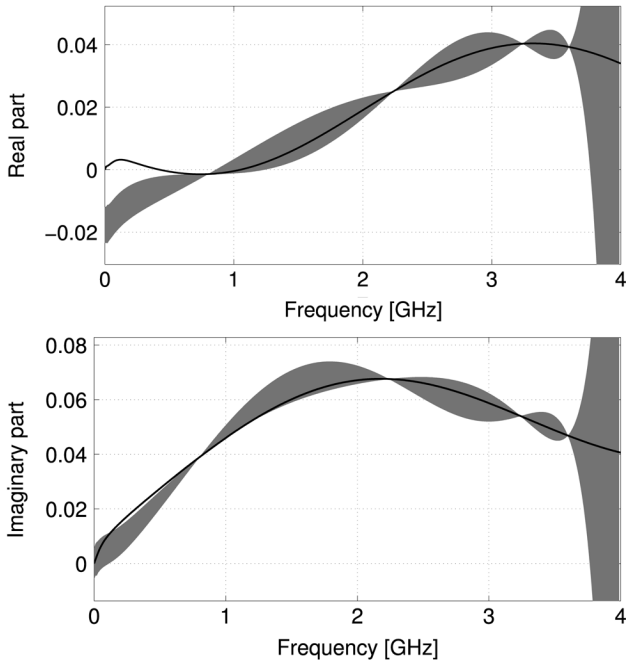

Fig. 9. Check for causality of S_{11}, based on computation of generalized Hilbert transform. Since continuous line (representing raw data) is outside gray area (computed Hilbert transform inclusive of a frequency-dependent error bar), dataset is noncausal.

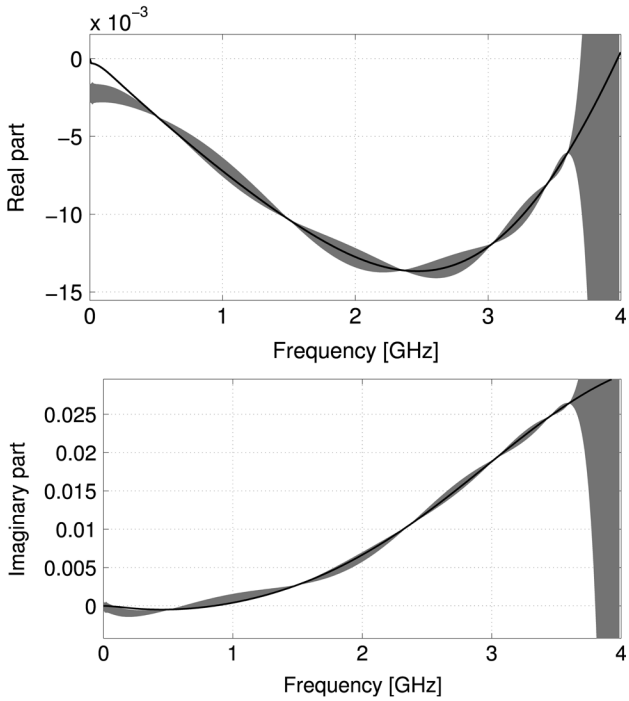

Fig. 10. As in Fig. 9, but for S_{24}.

Fig. 11. Layout of PCB with coupled interconnect structure under investigation. Port numbering is also specified.

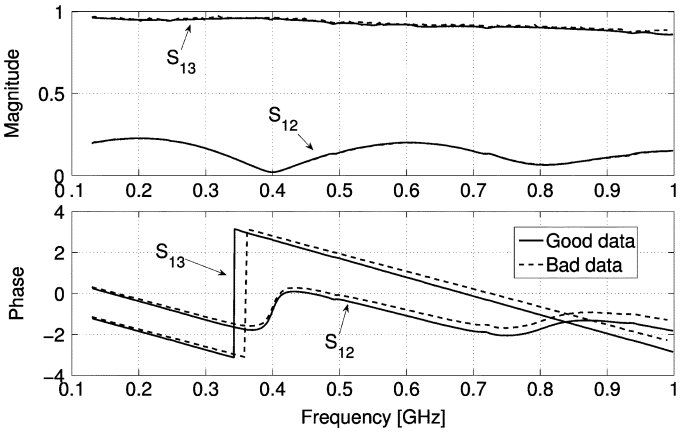

Fig. 12. Scattering parameters S_{12} (near-end crosstalk) and S_{13} (transmission) for two datasets of Section VI-C .

C. PCB Interconnect

We consider in this section a coupled interconnect structure on a printed circuit board (PCB), whose geometry is depicted in Fig. 11. We built a test board and we performed two sets of measurements of the four-port scattering matrix of the interconnect. The first measured dataset is valid and accurate. The second dataset is instead flawed by an imperfect calibration. Hence, we denote the former dataset as "good" and the latter as "bad." Magnitude and phase of two scattering matrix entries for the two measurements are compared in Fig. 12. Fig. 13 depicts the frequency-dependent maximum singular value of the two scattering matrices, showing that the "bad" dataset is also violating passivity (the maximum singular value is larger than one), whereas the "good" dataset is passive.

We now attempt the construction of a rational macromodel for these two datasets with a varying number of poles. The results obtained with VF are reported in Table IV, where three sets of models are compared. The models for the "good" and passive dataset are also passive and the VF error converges when the number of poles is increased. The models for the "bad" dataset are also convergent, but a passivity check, here performed using [54], shows that also the models are nonpassive. This is expected, since a model that closely matches a nonpassive dataset will almost surely be nonpassive. Finally, the set of models in the last column is obtained from the "bad" dataset by enforcing passivity, as in [54]. All these passive models are inaccurate with respect to the original data. This is also expected, since a passive model cannot match a nonpassive dataset better than a given threshold accuracy, which is of course related to the amount of passivity violation in the data. As a confirmation, the model accuracy seems to be limited to a value which is nearly the same as $\max_\omega\{\|S(j\omega)\| - 1\}$ (see Fig. 13). Note also that any other

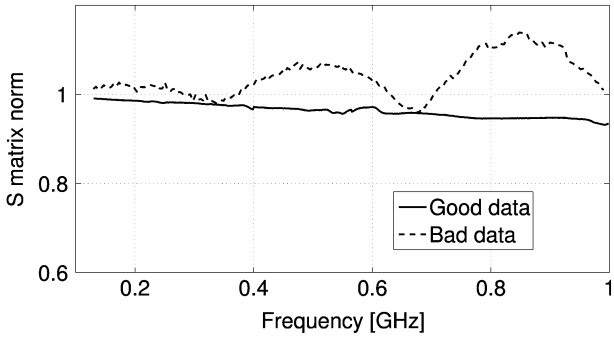

Fig. 13. Norm of S matrix: values greater than one denote passivity violations.

TABLE IV
MODEL ERRORS AS A FUNCTION OF NUMBER OF POLES

Model order	Passive data & models	Non-passive data & models	Non-passive data, passive models
6	0.240	0.280	0.23
12	0.020	0.020	0.11
18	0.012	0.017	0.13

passivity enforcement algorithm, such as [45], [52], will produce similar results.

The measured data for this example are only available from a minimum frequency $f_{\min} = 130$ MHz and not from dc. This fact has two important implications.

1) If we test data causality using the Kramers–Krönig dispersion relations (23), we need to take into account the unavoidable bias due to the missing samples. This is indeed the main motivation that led to the advanced algorithms in [40], [41], which explicitly deal with missing samples by computing an equivalent "numeric resolution" of the causality check. See [40] and [41] for details.
2) Any model derived from this data can only be accurate where frequency samples are available. Therefore, the model behavior from dc up to $f_{\min}$ is not under control, unless some additional assumptions on the missing data are made. This may lead to spurious passivity violations in the model, which are located at frequencies where raw data samples are missing.

In case only a "bad" nonpassive dataset is available, we are faced with three possibilities:

1) throw away the flawed dataset and repeat the measurement;
2) accept the accurate but nonpassive macromodel;
3) accept a passive macromodel at the cost of a reduced accuracy with respect to the available data.

It turns out that the first choice is the right one. In fact, an accurate but nonpassive model may lead to an unstable network even when suitable passive terminations are considered. This is actually not far from real life experience, and we show this for the nonpassive model with 18 poles. When we terminate the interconnect model with identical loads at its four ports with structure $R_1 \,\|\, (R_2 + j\omega L)$ (component values: $R_1 = 1.93\ \mathrm{k}\Omega$, $R_2 = 1.29\ \Omega, L = 9.18$ nH), we get the voltage waveform reported in Fig. 14, which confirms the loss of the network stability, caused by a pair of complex-conjugate poles with positive real part, $p_{1,2} = 0.037 \pm j5.40$ Grad/s. Thus, accepting nonpassive models involves a necessary risk that the system-level

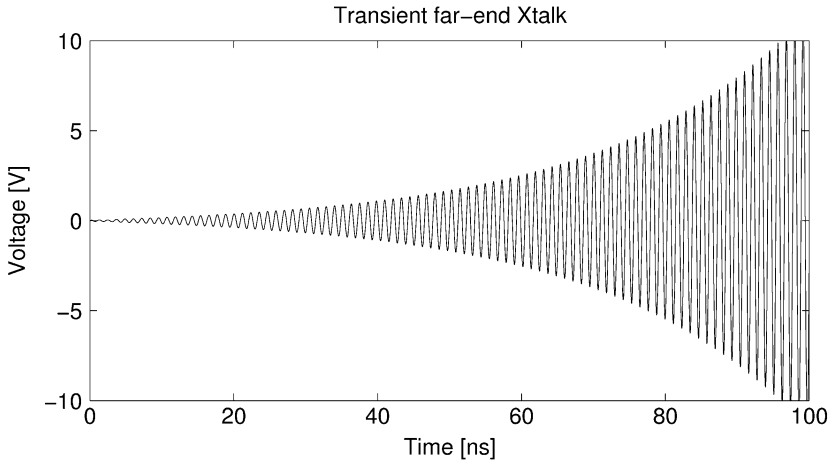

Fig. 14. Loss of stability of nonpassive model when connected to simple passive RL loads.

simulation employing the model may fail. The third choice has also some drawbacks. In fact, even if the model is passive, we will never know how closely it represents the real interconnect (which is certainly a passive structure), since it is derived from a dataset that does not represents correctly the fundamental physics of the system.

VII. Summary and Discussion

We have reviewed in this paper the fundamental properties of stability, causality, and passivity, and we have shown all important interrelations between them in the time, Laplace, and Fourier domains. These concepts have been used to interpret and justify common difficulties encountered when trying to derive macromodels from tabulated frequency data. We have shown with several test cases that whenever raw frequency data do not fulfill these fundamental properties, a failure in the macromodeling process must be expected.

The main conclusion of this work is twofold. First, it is mandatory that any dataset be certified to be self-consistent, causal, and passive before proceeding to further modeling steps. Second, any macromodeling algorithm must preserve such properties in order to avoid flawed simulation results. We conclude this paper by pointing the reader to a set of significant references on both data checking and consistent model extraction techniques.

We have shown that passivity is the strongest requirement, since it implies both causality and stability. When dealing with (scattering) frequency-domain tabulated data, we can apply Theorem V.3 to check for passivity. Unitary boundedness of the scattering matrix (condition 2) is easy to test, at least for the available samples. Conversely, checking dispersion relations (condition 1) is much more difficult. Only a few authors have considered this problem addressing the serious issues due to the tabulated nature of real data [35]–[39]. More recent results on robust causality check for bandlimited tabulated data can be found in [40] and [41].

The stability and the causality of rational (lumped) models based on poles-residues, poles-zeros, or state-space forms are easy to enforce. It is indeed sufficient to make sure that all poles have a (strictly) negative real part, as discussed in Section IV. The more difficult passivity enforcement reduces in this case to condition 2) of Theorems IV.3 and IV.4. For small-sized models the best approach is provided by a convex formulation of the passivity constraints via the positive real (PR) or the bounded real (BR) lemmas [42], [43], since these forms allow application of convex programming techniques for passivity enforcement [44]–[47]. Such techniques are guaranteed to find the optimal solution. Unfortunately, their computational complexity seriously impairs application to medium and large-sized models. These cases can be handled via suboptimal techniques based on linear or quadratic optimization [48]–[52] or Hamiltonian matrix perturbation [53]–[56].

Delay-based models (for, e.g., transmission lines) deserve special care [15]–[24]. Some techniques are available for model passivity enforcement by construction [21]. However, model size may grow for large delays, and model efficiency may be compromised. Very efficient models are available [15]–[20], but without the guarantee of passivity. Passivity enforcement for such models is still an open problem for future research [23], [24].

Acknowledgment

The authors are grateful to Dr. I. Kelander (NOKIA) for providing the data used in Section II, and to their colleagues I. Stievano, C. Siviero, V. Teppati, and G. Dassano for supplying the measurements used in Section VI-C.

References

[1] M. Nakhla and R. Achar, "Simulation of high-speed interconnects," *Proc. IEEE*, vol. 89, no. 5, pp. 693–728, May 2001.
[2] M. Celik, L. Pileggi, and A. Obadasioglu, *IC Interconnect Analysis*. Boston, MA: Kluwer, 2002.
[3] B. Gustavsen and A. Semlyen, "Rational approximation of frequency domain responses by vector fitting," *IEEE Trans. Power Delivery*, vol. 14, no. 3, pp. 1052–1061, Jul. 1999.
[4] A. Semlyen and B. Gustavsen, "Vector fitting by pole relocation for the state equation approximation of nonrational transfer matrices," *Circuits Syst. Signal Process*, vol. 19, no. 6, pp. 549–566, 2000.
[5] B. Gustavsen and A. Semlyen, "A robust approach for system identification in the frequency domain," *IEEE Trans. Power Delivery*, vol. 19, no. 3, pp. 1167–1173, Jul. 2004.
[6] C. K. Sanathanan and J. Koerner, "Transfer function synthesis as a ratio of two complex polynomials," *IEEE Trans. Automat. Contr.*, vol. 8, no. 1, pp. 56–58, Jan. 1963.

[7] W. Beyene and J. Schutt-Ainé, "Accurate frequency-domain modeling and efficient circuit simulation of high-speed packaging interconnects," *IEEE Trans. Microwave Theory Tech.*, vol. 45, no. 10, pp. 1941–1947, Oct. 1997.

[8] K. L. Choi and M. Swaminathan, "Development of model libraries for embedded passives using network synthesis," *IEEE Trans. Circuits Syst. II*, vol. 47, no. 4, pp. 249–260, Apr. 2000.

[9] M. Elzinga, K. Virga, L. Zhao, and J. L. Prince, "Pole-residue formulation for transient simulation of high-frequency interconnects using householder LS curve-fitting techniques," *IEEE Trans. Comp. Packag. Manufact. Technol.*, vol. 23, no. 1, pp. 142–147, Mar. 2000.

[10] M. Elzinga, K. Virga, and J. L. Prince, "Improve global rational approximation macromodeling algorithm for networks characterized by frequency-sampled data," *IEEE Trans. Microwave Theory Tech.*, vol. 48, no. 9, pp. 1461–1467, Sep. 2000.

[11] J. Morsey and A. C. Cangellaris, "PRIME: Passive realization of interconnects models from measures data," in *Proc. IEEE 10th Topical Meeting Electr. Perf. of Electron. Packag.*, 2001, pp. 47–50.

[12] S. Grivet-Talocia and M. Bandinu, "Improving the convergence of vector fitting in presence of noise," *IEEE Trans. Electromagnetic Compatibility*, vol. 48, no. 1, pp. 104–120, Feb. 2006.

[13] D. Deschrijver and T. Dhaene, "Broadband macromodeling of passive components using orthonormal vector fitting," *Electron. Lett.*, vol. 41, no. 21, pp. 1160–1161, Oct. 2005.

[14] *IdEM 2.4*, [Online]. Available: http://www.emc.polito.it

[15] F. H. Branin, "Transient analysis of lossless transmission lines," *Proc. IEEE*, vol. 55, pp. 2012–2013, 1967.

[16] A. J. Gruodis and C. S. Chang, "Coupled lossy transmission line characterization and simulation," *IBM J. Res. Development*, vol. 25, pp. 25–41, 1981.

[17] D. B. Kuznetsov and J. E. Schutt-Aine, "Optimal transient simulation of transmission lines," *IEEE Trans. Circuits Syst.—I*, vol. 43, no. 1, pp. 110–121, Jan. 1996.

[18] S. Lin and E. S. Kuh, "Transient simulation of lossy interconnects based on recursive convolution formulation," *IEEE Trans. Circuits Syst.—I*, vol. 39, no. 6, pp. 879–892, Jun. 1992.

[19] A. Semlyen and A. Dabuleanu, "Fast and accurate switching transient calculations on transmission lines with ground using recursive convolution," *IEEE Trans. Power Apparatus Syst.*, vol. 94, pp. 561–571, 1975.

[20] S. Grivet-Talocia, H. M. Huang, A. E. Ruehli, F. Canavero, and I. M. Elfadel, "Transient analysis of lossy transmission lines: An effective approach based on the method of characteristics," *IEEE Trans. Advanced Packaging*, vol. 27, no. 1, pp. 45–56, Feb. 2004.

[21] N. Nakhla, A. Dounavis, R. Achar, and M. S. Nakhla, "DEPACT: Delay extraction-based passive compact transmission-line macromodeling algorithm," *IEEE Trans. Adv. Packaging*, vol. 28, no. 1, pp. 13–23, Feb. 2005.

[22] R. Mandrekar and M. Swaminathan, "Causality enforcement in transient simulation of passive networks through delay extraction," in *Proc. 9th IEEE Workshop Signal Propagation on Interconnects, Garmisch-Partenkirchen, Germany*, May 10–13, 2005.

[23] E. Gad, C. Chen, M. Nakhla, and R. Achar, "A passivity checking algorithm for delay-based macromodels of lossy transmission lines," in *Proc. 9th IEEE Workshop on Signal Propagation on Interconnects*, May 10–13, 2005, pp. 125–128.

[24] E. Gad, C. Chen, M. Nakhla, and R. Achar, "Passivity verification in delay-based macromodels of electrical interconnects," *IEEE Trans. Circuits Syst.—I*, vol. 52, no. 10, pp. 2173–2187, Oct. 2005.

[25] A. H. Zemanian, "An N-port realizability theory based on the theory of distributions," *IEEE Trans. Circuit Theory*, vol. CT-10, pp. 265–274, Oct. 1963.

[26] M. R. Wohlers, *Lumped and Distributed Passive Networks*. New York: Academic, 1969.

[27] D. C. Youla, L. J. Castriota, and H. J. Carlin, "Bounded real scattering matrices and the foundations of linear passive network theory," *IRE Trans. Circuit Theory*, vol. CT-6, pp. 102–124, Mar. 1959.

[28] A. V. Oppenheim and A. S. Willsky, *Signals and Systems*. Englewood Cliffs, NJ: Prentice–Hall, 1983.

[29] A. H. Zemanian, "Realizability theory for continuous linear systems," in *Mathematics in Science and Engineering*. New York: Academic, 1972, vol. 97, pp. XV–231.

[30] E. J. Beltrami, "Linear dissipative systems, nonnegative definite distributional kernels, and the boundary values of bounder-real and positive-real matrices," *J. Math. Analysis Applic.*, vol. 19, pp. 231–246, 1967.

[31] H. A. Kramers, "La diffusion de la lumière par les atomes," in *Collected Scientific Papers*. Amsterdam, The Netherlands: North-Holland, 1956.

[32] R. Krönig, "On the theory of dispersion of x-rays," *J. Opt. Soc. Amer.*, vol. 12, pp. 547–557, 1926.

[33] N. M. Nussenzveig, *Causality and Dispersion Relations*. New York: Academic, 1972.

[34] E. C. Titchmarsh, *Introduction to the Theory of Fourier Integrals*, 2nd ed. London, U.K.: Oxford Univ. Press, 1948.

[35] G. W. Milton, D. J. Eyre, and J. V. Mantese, "Finite frequency range Kramers Krönig relations: Bounds on the dispersion," *Phys. Rev. Lett.*, vol. 79, pp. 3062–3065, 1997.

[36] K. R. Waters, J. Mobley, and J. G. Miller, "Causality-imposed (Kramers–Krönig) relationships between attenuation and dispersion," *IEEE Trans. Ultrason., Ferroelect., Freq. Contr.*, vol. 52, pp. 822–833, 2005.

[37] K. F. Palmer, M. Z. Williams, and B. A. Budde, "Multiply subtractive Kramers–Krönig analysis of optical data," *Appl. Opt.*, vol. 37, no. 13, pp. 2660–2673, May 1998.

[38] V. Lucarini, J. J. Saarinen, and K. Peiponen, "Multiply subtractive generalized Kramers-Krönig relations: Application on third-harmonic generation susceptibility on polysilane," *J. Chem. Phys.*, vol. 119, no. 21, pp. 11 095–11 098, Dec. 2003.

[39] F. M. Tesche, "On the use of the Hilbert transform for processing measured CW data," *IEEE Trans. Electromagn. Compat.*, vol. 34, pp. 259–266, 1992.

[40] P. Triverio and S. Grivet-Talocia, "A robust causality verification tool for tabulated frequency data," in *Proc. 10th IEEE Workshop Signal Propagation on Interconnects*, Berlin, Germany, May 9–12, 2006.

[41] P. Triverio and S. Grivet-Talocia, "On checking causality of bandlimited sampled frequency responses," in *Proc. 2nd Conf. Ph.D. Research in Microelectronics and Electronics (PRIME)*, Otranto, LE, Italy, June 12–15, 2006, pp. 501–504.

[42] K. Zhou, J. C. Doyle, and K. Glover, *Robust and Optimal Control*. Englewood Cliffs, NJ: Prentice–Hall, 1996.

[43] S. Boyd, L. El Ghaoui, E. Feron, and V. Balakrishnan, "Linear matrix inequalities in system and control theory," in *SIAM Studies in Applied Mathematics*. Philadelphia, PA: SIAM, 1994.

[44] S. Boyd and L. Vandenberghe, *Convex Optimization*. Cambridge, U.K.: Cambridge Univ. Press, 2004.

[45] C. P. Coelho, J. Phillips, and L. M. Silveira, "A convex programming approach for generating guaranteed passive approximations to tabulated frequency-data," *IEEE Trans. Computed-Aided Design Integrated Circuits Syst.*, vol. 23, no. 2, Feb. 2004.

[46] H. Chen and J. Fang, "Enforcing bounded realness of S parameter through trace parameterization," in *Proc. 12th IEEE Topical Meeting Electrical Performance of Electronic Packaging*, Princeton, NJ, Oct. 27–29, 2003, pp. 291–294.

[47] B. Dumitrescu, "Parameterization of positive-real transfer functions with fixed poles," *IEEE Trans. Circuits Syst.—I*, vol. 49, no. 4, pp. 523–526, Apr. 2002.

[48] B. Gustavsen and A. Semlyen, "Enforcing passivity for admittance matrices approximated by rational functions," *IEEE Trans. Power Syst.*, vol. 16, no. 1, pp. 97–104, Mar. 2001.

[49] R. Achar, P. K. Gunupudi, M. Nakhla, and E. Chiprout, "Passive interconnect reduction algorithm for distributed/measured networks," *IEEE Trans. Circuits Syst. II*, vol. 47, no. 4, pp. 287–301, Apr. 2000.

[50] D. Saraswat, R. Achar, and M. Nakhla, "Enforcing passivity for rational function based macromodels of tabulated data," in *Proc. 12th IEEE Topical Meeting Electrical Performance of Electronic Packaging*, Princeton, NJ, Oct. 27–29, 2003, pp. 295–298.

[51] D. Saraswat, R. Achar, and M. Nakhla, "A fast algorithm and practical considerations for passive macromodeling of measured/simulated data," *IEEE Trans. Components, Packaging and Manufacturing Technol.*, vol. 27, pp. 57–70, Feb. 2004.

[52] D. Saraswat, R. Achar, and M. Nakhla, "Global passivity enforcement algorithm for macromodels of interconnect subnetworks characterized by tabulated data," *IEEE Trans. VLSI Syst.*, vol. 13, no. 7, pp. 819–832, Jul. 2005.

[53] S. Grivet-Talocia, "Enforcing passivity of macromodels via spectral perturbation of hamiltonian matrices," in *Proc. 7th IEEE Workshop on Signal Propagation on Interconnects*, Siena, Italy, May 11–14, 2003, pp. 33–36.

[54] S. Grivet-Talocia, "Passivity enforcement via perturbation of Hamiltonian matrices," *IEEE Trans. Circuits Syst.—I*, vol. 51, no. 9, pp. 1755–1769, Sep. 2004.

[55] S. Grivet-Talocia and A. Ubolli, "On the generation of large passive macromodels for complex interconnect structures," *IEEE Trans. Adv. Packaging*, vol. 29, no. 1, pp. 39–54, Feb. 2006.

[56] S. Grivet-Talocia, "Improving the efficiency of passivity compensation schemes via adaptive sampling," in *Proc. 14th IEEE Topical Meeting Electrical Performance of Electronic Packaging*, Austin, TX, Oct. 24–26, 2005, pp. 231–234.

Piero Triverio (S'06) was born in Biella, Italy, in 1981. He received the Laurea Specialistica degree (M.Sc.) in electronics engineering, in 2005, from the Politechnic University of Turin, Italy, where he is currently pursuing the Ph.D. degree.

His research interests include the modeling and simulation of lumped and distributed interconnects and numerical algorithms.

Mr. Triverio was the recipient of the INTEL Best Student Paper Award presented at the IEEE 15th Topical Meeting on Electrical Performance of Electronic Packaging (EPEP 2006) and the OPTIME Award of the Turin Industrial Association. In 2005, he was selected for the IBM EMEA Top Student Recognition Event.

Stefano Grivet-Talocia (M'98–SM'07) received the Laurea and the Ph.D. degrees in electronic engineering from the Politechnic University of Turin, Italy.

From 1994 to 1996, he was at NASA/Goddard Space Flight Center, Greenbelt, MD, where he worked on applications of fractal geometry and wavelet transform to the analysis and processing of geophysical time series. Currently, he is an Associate Professor of Circuit Theory with the Department of Electronics, Polytechnic of Turin. His research interests include passive macromodeling of lumped and distributed interconnect structures, modeling, and simulation of fields, circuits, and their interaction, wavelets, time-frequency transforms, and their applications. He is the author of more than 80 journal and conference papers.

Dr. Grivet-Talocia served as Associate Editor for the IEEE TRANSACTIONS ON ELECTROMAGNETIC COMPATIBILITY from 1999 to 2001.

Michel S. Nakhla (S'73–M'75–SM'88–F'98) received the M.A.Sc. and Ph.D. degrees in electrical engineering from University of Waterloo, Ontario, Canada, in 1973 and 1975, respectively.

From 1976 to 1988 he was with Bell-Northern Research, Ottawa, Canada, as the Senior Manager of the computer-aided engineering group. In 1988, he joined Carleton University, Ottawa, Canada, as a Professor and the holder of the Computer-Aided Engineering Senior Industrial Chair established by Bell-Northern Research and the Natural Sciences and Engineering Research Council of Canada. He is a Chancellor's Professor of Electrical Engineering at Carleton University. He is the Founder of the high-speed CAD research group at Carleton University. He serves as a technical consultant for several industrial organizations and is the principal investigator for several major sponsored research projects. His research interests include modeling and simulation of high-speed circuits and interconnects, nonlinear circuits, multidisciplinary optimization, thermal and electromagnetic emission analysis, MEMS and neural networks. Also, he has also served as a member of many Canadian and international government-sponsored research grants selection panels.

Dr. Nakhla serves on various international committees, including the standing committee of the IEEE International Signal Propagation on Interconnects Workshop (SPI), the technical program committee of the IEEE International Microwave Symposium (IMS), the technical program committee of the IEEE Topical Meeting on Electrical Performance of Electronic Packaging and the CAD committee (MTT-1) of the IEEE Microwave Theory and Techniques Society. He is an Associate Editor of the IEEE TRANSACTIONS ON ADVANCED PACKAGING and served as Associate Editor of the IEEE TRANSACTIONS ON CIRCUITS AND SYSTEMS and as Associate Editor of the *Circuits, Systems and Signal Processing Journal*.

Flavio G. Canavero (M'90–SM'99–F'04) received the electronic engineering degree from Politecnico (Technical University) of Torino, Italy, and the Ph.D. degree from the Georgia Institute of Technology, Atlanta, GA, in 1986.

Currently, he is a Professor of Circuit Theory with the Department of Electronics, Politecnico di Torino. His research interests include signal integrity and EMC design issues, interconnect modeling, black-box characterization of digital integrated circuits, EMI, and statistics in EMC.

Dr. Canavero has been the Editor-in-Chief of IEEE TRANSACTIONS ON ELECTROMAGNETIC COMPATIBILITY. He is Chair of URSI Commission E, Editor of the Practical Papers Section of the EMC Newsletters, and Organizer of two IEEE Workshops in 2007 (Signal Propagation on Interconnects and European Systems Packaging Workshop).

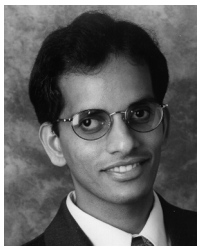

Ramachandra Achar (S'95–M'00–SM'04) received the B.Eng. degree in electronics engineering from Bangalore University, Bangalore, India, in 1990, the M.Eng. degree in microelectronics from Birla Institute of Technology and Science, Pilani, India, in 1992, and the Ph.D. degree from Carleton University, Ottawa, ON, Canada, in 1998.

He spent the summer of 1995 working on high-speed interconnect analysis at T. J. Watson Research Center, IBM, Yorktown Heights, NY. He was a graduate trainee at Central Electronics Engineering Research Institute, Pilani, India, during 1992 and was also previously employed at Larsen and Toubro Engineers Ltd., Mysore, India, and at Indian Institute of Science, Bangalore, as an Research and Development Engineer. During 1998 to 2000, he served as a Research Engineer in the CAE Group, Carleton University. He is currently an Associate Professor in the Department of Electronics, Carleton University. His research interests include signal integrity analysis, numerical algorithms, and the development of computer-aided design tools for modeling and simulation of high-frequency interconnects, nonlinear circuits, microwave/RF networks, optoelectronic devices, MEMS, and EMC/EMI. He has published over 100 peer-reviewed articles in international journals/conferences, six multimedia books on signal integrity, and five chapters in different books. He is a practicing professional engineer in the Province of Ontario, Canada.

Dr. Achar is a recipient of several prestigious awards, including the University Research Achievement Award (2004), Natural Science and Engineering Research Council (NSERC) Doctoral Medal (2000), Medal for the Outstanding Doctoral Work (1998), Strategic Microelectronics Corporation (SMC) Award (1997), Canadian Microelectronics Corporation (CMC) Award (1996). Also, he and several of his students have won best student paper awards in premier IEEE conferences such as EPEP and IMS. He serves on the technical program committee as a member as well as track chair of several leading IEEE conferences and is a consultant for several leading industries focused on high-frequency circuits, systems, and tools. He is the Chair of the joint chapters of CAS/EDS/SSC societies of the Ottawa IEEE section.